

## Study of Seasonal Rainfall Infiltration Via Time-Lapse Surface Electrical Resistivity Tomography: Case Study of Gamboa Area, Panama Canal Watershed

Alexis Mojica<sup>1</sup>, Irving Díaz<sup>2</sup>, Carlos A. Ho<sup>1</sup>, Fred Ogden<sup>3</sup>, Reinhardt Pinzón<sup>4</sup>, José Fábrega<sup>4</sup>, David Vega<sup>4</sup> and Jan Hendrickx<sup>5</sup>

<sup>1</sup>Laboratorio de Investigación en Ingeniería y Ciencias Aplicadas, Centro Experimental de Ingeniería, Universidad Tecnológica de Panamá, Panama City, Panama. <sup>2</sup>Facultad de Ingeniería Mecánica, Universidad Tecnológica de Panamá, Panama City, Panama. <sup>3</sup>Department of Civil & Architectural Engineering, College of Engineering and Applied Science, University of Wyoming, Laramie, Wyoming, USA. <sup>4</sup>Centro de Investigaciones Hidráulicas e Hidrotécnicas, Universidad Tecnológica de Panamá, Panama City, Panama. <sup>5</sup>Department of Earth & Environmental Science, New Mexico Tech, Socorro, New Mexico, USA.

**ABSTRACT:** The present investigation was focused on the variations in rainwater infiltration experienced by soils of Gamboa zone (Panama Canal Watershed) during various seasons of the year, employing a time-lapse analysis of electrical resistivity tomography (ERT). In 2009, a total of 3 geoelectrical tests were undertaken during the dry, transition and rainy seasons across a profile 47 m in length, strategically distributed on site. The results obtained in this study showed strong variations in calculated resistivity between these seasons, taking the dry season as a reference with decreases and increases of percent difference of resistivity between -20% and -100%, and between 50% and 100%, respectively. These decreases, when displayed through a sequence of time-lapse images, reveal a superficial extension of the water content variations along the entire profile, as well as strong inversion artifacts showing false increases of calculated electrical resistivity. Decreases are the product of the rainfall increase obtained in this type of tropical environment; permanent conductive anomalies in 3 tests are associated with the streams close to the study site. The results of this work were compared with a simulation resulting from a series of bidimensional models applied to the 3 studies evaluated: dry, transition and rainy seasons.

**KEYWORDS:** apparent resistivity, ERT, rainfall, time-lapse analysis, inversion artifact, Gamboa, modeling

**CITATION:** Mojica et al. Study of Seasonal Rainfall Infiltration Via Time-Lapse Surface Electrical Resistivity Tomography: Case Study of Gamboa Area, Panama Canal Watershed. *Air, Soil and Water Research* 2013;6: 131-139 doi:10.4137/ASWR.S12306.

**TYPE:** Original Research

**FUNDING:** The authors want to thank the "Secretaría Nacional de Ciencia y Tecnología (SENACYT)" for the support given to this important project.

**COMPETING INTERESTS:** Author(s) disclose no potential conflicts of interest.

**COPYRIGHT:** © the authors, publisher and licensee Libertas Academica Limited. This is an open-access article distributed under the terms of the Creative Commons CC-BY-NC 3.0 License.

**CORRESPONDENCE:** alexis.mojica@utp.ac.pa

### Introduction

In recent years, society has been attending to the urgent necessity to develop tools able to characterize, monitor and investigate various parameters and hydrogeologic processes that take place at the upper layers of our planet.<sup>1</sup> This initiative is related to the conservation of natural sources for water, which support local ecosystems and the world economy. These resources are strongly challenged by climatic factors that are consequences of human activities over soils and forests. In some tropical countries, groundwater

sources provide drinking water to their population. Use of these sources depends on the rainy season, which starts the recharge process. The Panama Canal is one of the most important maritime routes at a global level. The Canal allows for a rapid communication between the Atlantic and Pacific oceans, making a more dynamic commercial and economic exchange among world nations. Due to this, the understanding and conservation of water resources in the Panama Canal Watershed has become one of the most important priorities regarding their operation, without excluding the water



employed for consumption by human settlements located at the Panama Canal riverbanks.

In response to the need for a better understanding of the source of this important natural resource, the field of hydrogeophysics has emerged as a science that investigate a diverse number of hydrological processes employing geophysical techniques. Today, there is an extensive list of references about the applicability of these techniques to the study of groundwater; as examples, we can refer to the work of Williams et al,<sup>2</sup> Haeni,<sup>3</sup> Annan,<sup>4</sup> Steeples,<sup>5</sup> Ekinici et al<sup>6</sup> and Robinson et al.<sup>7</sup> Nevertheless, among all the existing geophysical techniques, the electric and electromagnetic are more widely applied for this kind of research.<sup>8</sup> As examples we can mention the works of Sandberg et al,<sup>9</sup> Louis et al,<sup>10,11</sup> Giudici et al,<sup>12</sup> Braga et al,<sup>13</sup> Robineau et al,<sup>14</sup> and Yeh et al.<sup>15</sup> For the electrical prospection, the time-lapse analysis of electrical resistivity tomography (ERT) has been often used in studies related to the monitoring of groundwater at different seasons.<sup>16-19</sup>

This geophysical prospection work is framed within a project focused on studying the effect of seasonal rainfall over the groundwater volumes at the Panama Canal Watershed, specifically at a small site in the Gamboa area (Fig. 1). This work is focused on how superficial infiltrations produced by rainfall affect the electrical resistivity distribution in the subsoil during the dry, transition and rainy seasons (2009), employing a time-lapse ERT method along a profile of 47 m of length.

Finally, the primary objective was to understand the effect produced by those infiltrations on the results of electrical resistivity tomographies. 3 superficial infiltration scenarios were recreated that correspond to the given seasons and their translations in sets of apparent electrical resistivity synthetic data, employing an algorithm based in a finite difference approximation.<sup>20</sup>

### The Site

The Isthmus of Panama has a warm, wet tropical climate with a cycle of rainfall determined by moisture from the Caribbean and the continental divide, which acts as a rain-shield for the Pacific lowlands. Panama has no seasons characterized by changes in temperature but has a rainy and dry seasons; the transition at the end of the dry season to the beginning of rainy season is associated with the disappearance of trade winds.

The Panama Canal watershed rests over the tectonic limit from between the Choco and Chorotega blocks that together make the Panamanian subplate.<sup>21</sup> Following Mann<sup>22</sup> the origin of this sub-plate is related to the subsidence of various oceanic plates that took place during the Cretaceous and Cenozoic era. The work of Jones,<sup>23</sup> Terry,<sup>24</sup> Woodring,<sup>25</sup> Stewart et al,<sup>26</sup> and Escalante<sup>27</sup> has postulated that a dense sequence of sediments and volcanic rocks characterize the Panama Canal Watershed, which lasted from the Eocene to the Pleistocene.

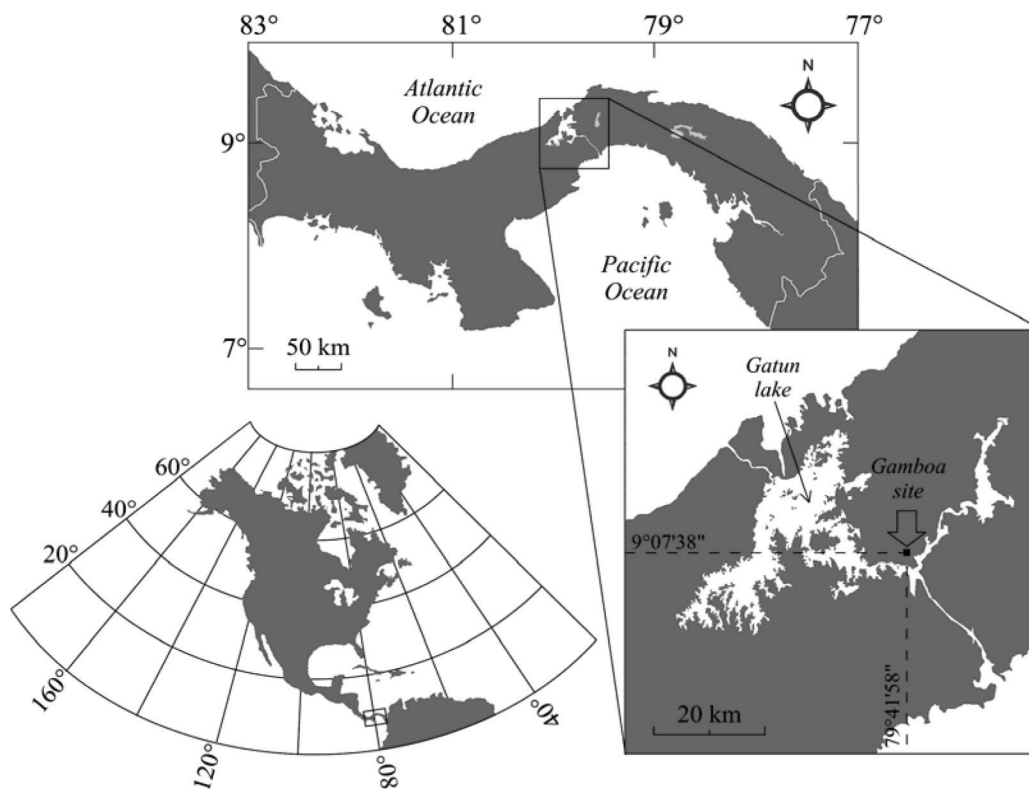
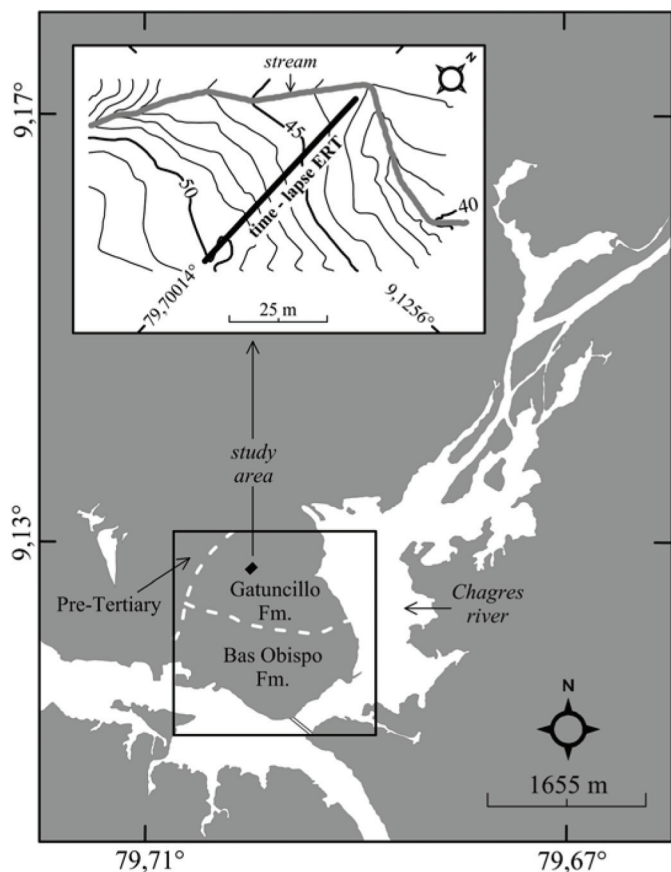


Figure 1. Geographic location of the Gamboa area at the Panama Canal watershed.



**Figure 2.** Study area location and profile distribution at the Gamboa area, Panama Canal watershed.

The site rests over the eocenic Gatuncillo formation (Fig. 2) corresponding to a sedimentary unit of greater deep; this means that the soils in this area are meteorized from sedimentary material. Because of the originating material, they have a low level of acidity and high level of organic matter (humus). The geologic elements that characterize this formation are limestone, sandstone, shale stone and foraminifera; according to Woodring,<sup>25</sup> Stewart et al,<sup>26</sup> and Escalante,<sup>27</sup> this formation rests in a discontinuous manner over the Pre-tertiary volcanic basement. Under this formation, we find the Bas Obispo formation, which is characterized by the presence of agglomerates and hard tuffs.

The site is located at the lower part of a steep area whose altitude range spans from 30 to 223 m over sea level. This zone, known as Cerro Pelado, is drained by a series of small streams all year around.<sup>28</sup> In the Northern part of Cerro Pelado, 3 streams have been identified. One of them does not flow during the dry season. Regarding the climatic site condition, it is important to mention that the intertropical conveying zone, together with the site topography, controls greatly the rainfall at the site of interest and at the Isthmus,<sup>29</sup> where the rainy season generally commences from May to December and the dry season lasts from the end of December to the end of April. According to Niedzialek,<sup>28</sup> in addition to this,

Panama has a precipitation gradient from the Caribbean to the Pacific. The Caribbean side gets more rainfall, due to the trade winds charged with humidity that originate mainly from the northwest during the dry season. Gamboa is found almost at the center of the Panama Isthmus, and shows a strong season-oriented precipitation with an annual average of 2148 mm. We propose that the zone of interest shows the optimum conditions for the development of a groundwater monitoring that is focalized on geophysical prospection.

For the current project, March was chosen because the low level of rain (dry season), and as a reference for geophysical survey; for the rainy season, October was chosen because it is the period of greatest precipitation rate. June represents the transition season, a very important period for geophysical survey because shows the changes in the electrical properties of the subsoil that occur between the dry and rainy seasons. Geophysical surveys were carried out on March 12 (dry season), June 4 (transition season) and October 30 (rainy season).

## Methods

**Electrical methods.** Electrical methods involved measuring the electrical resistivity (in  $\Omega\text{m}$ ), or its inverse, electrical conductivity, for a bulk volume of soil; the electrical resistivity is a measure of how much the soil resists the flow of electrical charges. The electrical properties of rocks and minerals are controlled by chemistry and thermodynamic parameters such as pressure and temperature in the medium in which the electrical charges moves;<sup>30</sup> the mobility of these charges are governed by the electrolytic fluid conduction of the fluid content at the porous saturated rocks and depends on their petrophysical properties. The electronic and the electrolytic conductivity of the soil loosely depends on the temperature and pressure. Some minerals act like insulators at room temperature, then their electrical conductivity is low. So, the semiconduction phenomenon is presented.

The electrical method used in the current study is characterized by the use of 2 current and 2 voltage electrodes, partially inserted at the ground surface. These parameters (voltage, in V, and current, in A), in conjunction with electrode spacing can be used to calculate the apparent resistivity of the soil. ERT is an electrical technique for imaging or estimating the distribution of electrical resistivity in the subsoil, from apparent resistivity data made at the surface. At the field level, a series of electrode are attached to the resistivity meter for data collection. The measurement is repeated for other consecutive electrodes and completes the first depth layer. This procedure is then repeated with greater separations among electrodes. This set of characteristics, in addition to its non-invasive character, makes the electrical method a favorable technique due to its sensibility to saturated porous spaces. In this context, the ERT constitutes a relatively recent modality of electrical prospection that has been applied extensively in hydrogeological studies.<sup>31</sup>



**Apparent resistivity data inversion process and time lapse analysis.** This measured apparent electrical resistivity data can be represented under the shape of a pseudo-section, which shows variations in data as a function of electrode separation and not from the real depth. Only an inversion process of the apparent electrical resistivity data will give as a result a more precise subsoil image.<sup>32</sup> This image is obtained by determining a terrain model that provides reliable data measures, subject to certain restrictions.<sup>33</sup> From the measured apparent resistivity data, an initial resistivity model is constructed; later, a direct modeling process based on the initial model is made to calculate the predicted apparent resistivity values. Then, these values are compared with measured data and if there is no correspondence with the expected results, the initial model is modified and the process is repeated until the problem is solved. In summary, the resistivity inversion is focused to find a resistivity model whose response  $\rho_i$  best fits the measured apparent resistivity data  $\rho_{(ap)i}$ . The goodness of fit of this model is characterized by the RMS error:

$$RMS = 100 \left[ \left\{ \sum_{i=1}^n \left( \rho_i - \rho_{(ap)i} \right) / \rho_{(ap)i} \right\}^2 \frac{1}{n} \right]^{1/2} \quad (1)$$

where  $n$  corresponds to the number of measured data. The time-lapse ERT method is used for in-situ monitoring applications; when the electrodes are inserted along the profile, then a base apparent resistivity dataset is collected and inverted; subsequently, the survey is repeated during the period of monitoring. In time-lapse inversion scheme, the inversion output file of the first dataset is served as the input of the time-lapse inversion; the subsequent apparent resistivity datasets are inverted, with the base inversion results as the a-priori information. The algorithm inverts the difference between each dataset and the base dataset; the result of time-lapse inversion is presented as the percent difference between the 2 sections.<sup>34</sup>

**Experimental device.** A total of 3 apparent resistivity data sets were obtained from the profile (Fig. 2), corresponding to the dry, transition and rainy seasons (between March and October 2009) using 48 electrodes, regularly spaced at 1 m intervals. These datasets correspond to the dry, transition and rainy seasons, with a total of 15 depth layers. This electrode distribution was chosen due to area boundaries and to get a good resolution in the upper layers. The acquisitions were made with a 400 V prototype in the output, which is composed of a stabilizer, oscillator and power system, using a 360 quadripoles Wenner- $\alpha$  sequence. This instrument works together with a switch that interconnects the electrodes so that they are systematically distributed in a longitudinal profile. For the Wenner- $\alpha$  array survey employed in this study, the electrical current runs through a pair of external electrodes and the voltage is measured with another pair of internal electrodes.

It is important to point out that the array selection has several advantages over other array types; these advantages include (i) an intermediate range of depth, (ii) an intermediate resolution, and (iii) a moderated sensitivity to geological noise Barker.<sup>35</sup> In addition, as Guérin et al<sup>36</sup> pointed out, the final output of this array is a smooth signal. According to some authors, for time-lapse ERT experiments, using Wenner- $\alpha$  array can give good results. It is noteworthy that after each test, the electrodes were removed due to the long period between these geophysical tests.

**The forward modeling.** With the aim of investigating the effect generated by the infiltrations produced by rainfall and the streams close to the site of interest over the ERT results obtained throughout the year, a total of 3 scenarios were constructed, taking as reference the interpretations realized over the experimental results and the stratigraphic information available. For the 2D modeling of these scenarios an algorithm based on the finite difference method was used, in which the subsoil was divided into a set of cells with a rectangular grid.<sup>37</sup> This method allows for determination of the electrical potential  $\Phi$  (in V) in each one of the node within the grid. The mathematical expression relating potentials and the electrical current  $i$  (in A) is given by:

$$-\nabla \cdot (\sigma \nabla \Phi) = i \delta (r - r_s) \quad (2)$$

Dirac Delta function  $\delta$  employed in this equation indicates that the charge density only varies at the electrical current source injection point located in  $(r - r_s)$ . The electrical resistivity models established for each one of the corresponding scenarios (dry, transition and rainy seasons) were evaluated employing modeling software called Res2Dmod.<sup>20,37</sup> The corresponding set of synthetic values of apparent electrical resistivity were obtained, defining a Wenner- $\alpha$  array with an electrode separation of 1 m, with an addition of 2% of Gaussian noise. Each of these datasets was also inverted and employed the time-lapse inversion criteria used for field data.

## Results and Discussion

**ERT profile.** The program used for this study to solve the inverse problem was the EarthImager 2D from AGI Advanced. This program employs the L2-norm (smooth model inversion) as one of the versions of the least squares optimization method present in the program; this version (Occam's inversion) finds the smoothest possible model whose response fits the data to an a-priori Chi-squared statistic.<sup>34</sup> This version was adopted taking into consideration possible levels of infiltration and geological elements present in the study area.

The apparent resistivity datasets measured during the seasons of interest are presented graphically with the pseudo-sections in Figures 3(a), (c) and (e). The results from the time-lapse inversion process completed on these data sets are displayed in the tomographies from Figures 3(b), (d) and (f); the number of

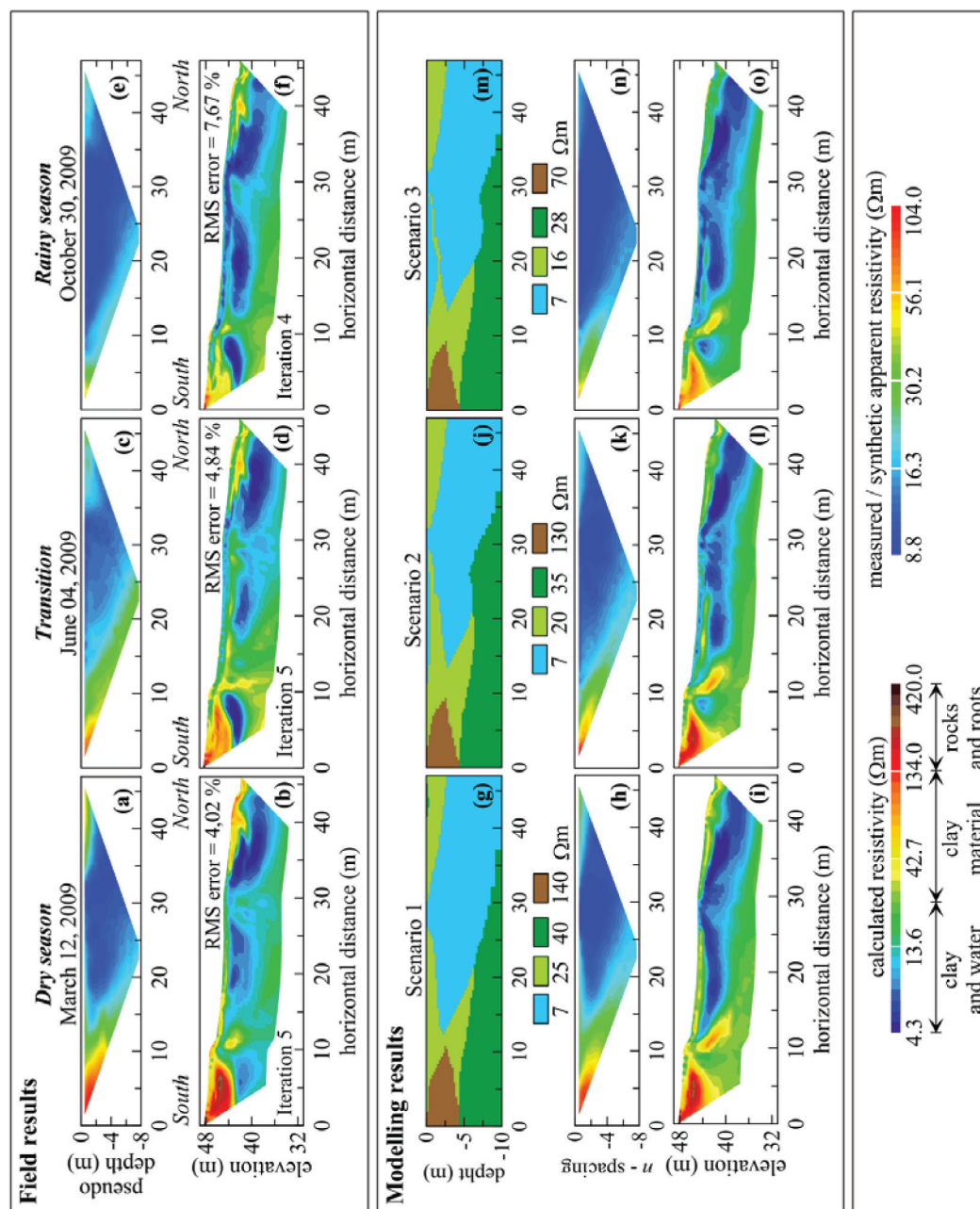


**Figure 3.** Pseudo-sections of measured (a, b and c) and synthetic (h, k and n) apparent resistivity from theoretical scenarios (g, j and m) associated with dry, transition and rainy seasons and interpreted resistivity section for field (b, d and f) and synthetic data (i, l and o), via time-lapse analysis.

iterations and RMS errors for each test are shown in Table 1. In these results we can identify a total of 3 horizons: the first horizon is characterized by a blue/light blue tone, with a calculated electrical resistivity extending from 4.3 to 13.6  $\Omega\text{m}$ . In the Figure 3(b) this horizon is unable to extend up to the surface due to the lack of rain in this season, but it is possible to identify this horizon in depth due to the infiltration through the clay layer by the stream water that is located in Northern part close to the site of interest (Fig. 2). In Figure 3(d), the horizon is able to extend up to a surface between 14 and 35 m along the profile, with depths no greater than 1 m. This superficial extension is strongly related to the first rainfall events

occurring in the site, which are associated with the transition period between dry and rainy seasons; this superficial horizon is associated with the infiltration process of these first rains through the humus layer. This superficial layer has been identified by the stratigraphic information obtained from the drillings made close to the profile. In this result, it is still possible to identify water infiltration caused by the stream. In the Figure 3(f), this horizon occupies a great part of the space extending to the surface between 6 and 40 m along the profile. In this Figure, the past scenario is repeated but with a more noticeable contribution from the characteristic season rainfalls through the superficial layer.

**Table 1.** Meteorological information periods of geophysical surveys, number of iterations, and RMS error after time-lapse ERT inversion process for each test.

SEASON	DATE	PRECIPITATION (MM)	AIR TEMPERATURE (°C)	ITERATION N°	RMS ERROR (%)
Dry	March 12	0	26.3	5	4.02
Transition	June 4	48	26.5	5	4.84
Rainy	October 30	88	26.3	4	7.67

The second horizon is represented by a green/yellow tone, with calculated electrical resistivity values ranging from 13.6 to 75.7  $\Omega\text{m}$ . This horizon is associated with clayish material. Figure 3(b) shows that this horizon represents a superficial layer extending along the whole profile. During the transition season (Fig. 3(d)), the surface layer is defined in part as a conducting horizon product of the first rains. In the rainy season (Fig. 3(f)), this horizon is reduced due to the conducting horizon extension, but defined in depth due to the presence of dense clay material.

The third horizon is represented by a resistant anomaly in orange/red tone with a resistivity range extending from 75.7 to 420.0  $\Omega\text{m}$ . This anomaly is associated with an accumulation of rocks and roots. In Figure 3(b), it can be seen that this anomaly extends up to 8 m along the profile with a vertical extension of 4.5 m. The Figure 3(d) shows that this anomaly seems to maintain its geometry but with values below the resistivity, as a result of the first rains that take place during the transition season, becoming weaker in Figure 3(f). The greater part of the space initially occupied by this strong anomaly is represented during the rainy season by electrical resistivity values with characteristics of the first 2 horizons. The dimension reduction of this anomaly is due to the water accumulation taking place at this time of the year.

**Synthetic data.** To understand the effect produced by the superficial infiltrations generated by rains and the existing streams close to the profile, 3 theoretical scenarios were tested with characteristics similar to the ones found to the dry, transition and rainy seasons. The different types of models and parameters employed in this study are shown in scenarios of the Figures 3(g), (j) and (m). In first scenario, a light blue tone (7  $\Omega\text{m}$ ) represents in depth the strong humidity caused by the stream, and in the second and third scenario we have a surface layer with the same electrical resistivity value representing the infiltration process in the humus layer as a contribution of rainfall during the transition and in the rainy seasons, respectively. In all scenarios, light green, green and brown tones represent the clay material, dense clay material and roots and rock accumulations, respectively whose electrical resistivity values tend to decrease by increasing moisture over time.

Figures 3(h), (k) and (n) correspond to the pseudo-sections of synthetic apparent resistivity generated from each model with 2% of Gaussian noise, and Figures 3(i), (l) and (o) are the synthetic tomographies corresponding to the inverted resistivity models employing the time-lapse

inversion criteria with the smooth method as an inversion technique for the first stage.

#### Time-lapse analysis (field and modeling results).

Figures 4(a) and (b) show the time-lapse analysis results as a percent change in resistivity from March 12 to June 4 (dry-transition seasons), and March 12 to October 30 (dry-rainy seasons), respectively.

These images allow us to identify the increments ( $\% > 0$ ) and reductions ( $\% < 0$ ) that the calculated electrical resistivity values exhibit for different temporal periods. Between March 1 to 11, 2009 only 14 mm of precipitation were obtained in the site, with 0 mm for March 12 (first test). These meteorological data are characteristic of this season of the year. Starting the last days of April, the first rains showed, between this period and June 3 (characteristic of the transition season) 254 mm of rainfall were registered with 48 mm for June 4 (see Table 1).

In between this date and October 30, the rainfall levels were high, characteristic of the rainy season, registering a total of 1512 mm of rain with 88 mm for October 30. For the 2 time periods in 2009, which are defined by 3 dates where the electrical tomographies were developed, the air temperature differences were similar and no greater than 0.20°C; Table 1 shows the air temperature values for these periods. Figure 5 shows the average total daily precipitation and main air temperature registered by a meteorological station located in Gamboa, for the year 2009.

Relative to the time-lapse ERT analysis obtained in Figures 4(a) and (b), we can establish the following patterns: In Figure 4(a), a strong decrease in the calculated electrical resistivity values ( $-20\% \rightarrow -100\%$ ) can be observed in the shape of an almost superficial continuous layer of black tone extending throughout the profile, with a vertical extension ranging in between 0.70 up to 1.20 m, but between 0 and 8 m a strong decrease in electrical resistivity is observed, occupying an irregular area with a vertical extension up to 5.8 m. In Figure 4(b), the decrease in calculated resistivity values is reflected more noticeably in the superficial layer, with a vertical extension ranging between 1.10 and 1.45 m. In the profile south section (0–9 m), the decrease is greater in dimension to the last result. These decreases are linked to the rains that began in May and lasted until the end of November according to weather information mentioned above.

In Figures 4(a) and (b) 2 strong increases in the calculated resistivity values are clearly observed. Both increases

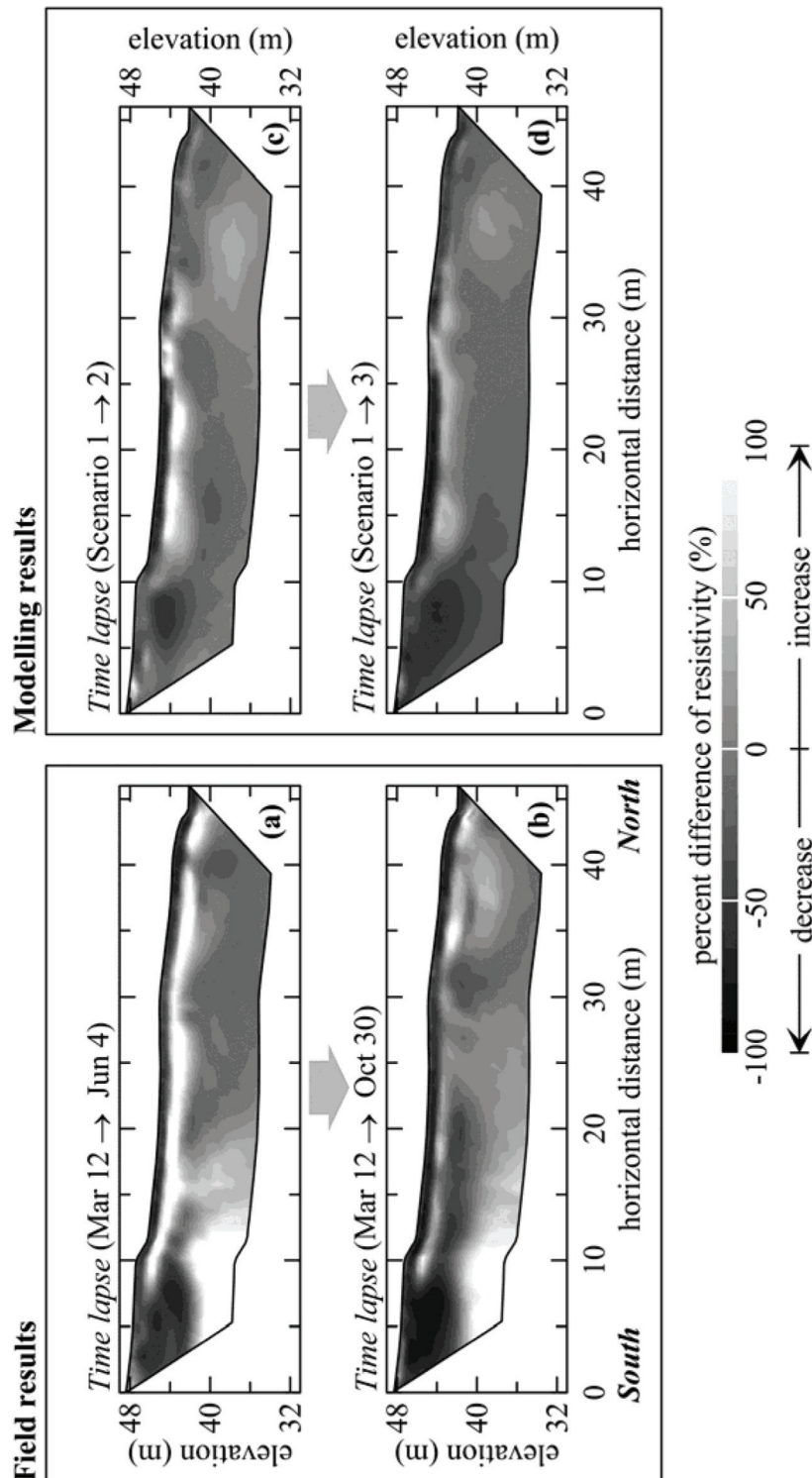


**Figure 4.** Percent change in resistivity from the dry season to: (a) the transition and (b) the rainy seasons, and percent change in resistivity obtained from the synthetic data from the Scenario 1 to: (c) the Scenario 2 and (d) 3.

are represented by a white tone which percent difference of resistivity is extended from 50% to 100%. In Figure 4(a) the extension of the first increase is defined in a zone between 7 and 47 m along the profile, and the vertical extension ranges from 0.70 to 4.0 m. The second increment extends between

0 and 10 m along the profile and at a depth between 5 and 7 m. In this result, these strong increases can be associated with time-lapse artifacts that are linked to the tendency to remove and relocate the electrodes for each test at the profile. In addition another causes are some noise levels and the

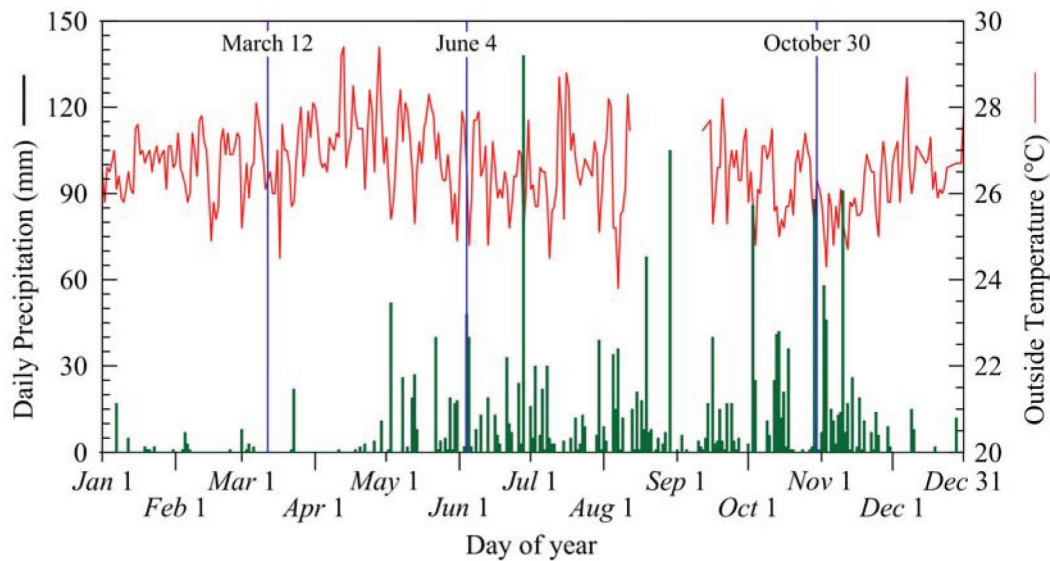


**Figure 5.** Average total daily rainfall and average air temperature registered in 2009 at the Gamboa area and days of geophysical surveys (Source: Panama Canal Authority).

inversion process; these negative effects has been reported by some authors.<sup>38,39</sup> Figure 4(b) shows a reduction in extension of these time-lapse artifacts.

The light grey tone zone is characterized by presenting weak variations in the calculated electrical resistivity values between the transition and rainy seasons in relation to the dry season. This area of low resistivity variation occupies a considerable area with respect to increasing and decreasing zones.

A comparison of the last modeling results with respect to the results obtained in Figures 3(b), (d) and (f), show that the established models for the representation of each scenario adjust positively to the reality of this important tropical zone at the Panamanian Isthmus, where the water contributed from streams (in dry season) and rains (in transition and rainy seasons) constitute the main sources feeding the area. Percent difference in resistivity images of these results (Figs. 4(c) and (d)) show strong decreases in superficial layer ( $<-50\%$ ) in black tone that can be compared with results of Figure 4(a) and (b). An increase area ( $>50\%$ ) in white tone just below the surface layer described above is presented. The remaining space presents very low percent differences of resistivity ( $\sim 0\%$ ), so white tone areas of Figures 4(a) and (b) (located in depth, at the beginning of the profile) are not shown in this result.

## Conclusions

In an effort to understand the processes taking place in the subsoil, the time-lapse ERT method could become a useful tool for monitoring changes in the physical properties of soils in tropical areas. The strong variation exhibited by the subsoil electrical properties in the Panama Canal Zone shows the important seasonal changes occurring in the tropics, where the decrease in percent differences of resistivity of the subsoil is closely related to the superficial infiltration produced by the rainfall starting during

the transitional season through the rest of the year. Throughout the year, contribution to the groundwater from stream infiltration close to the site is also noticeable. However, according to the geophysical monitoring in this study, the greater contribution of this important water resource comes from the rainfall events through the humus layer; soils that characterize this region have a vertical pore system created by the plant roots and lumbricid action. Another important aspect is the land cover of the site, which reduces soil temperature and thus the water evaporation. The strong increases in the subsoil electrical resistivity values that have been identified in this study can be associated with inversion artifacts linked to the removal of the electrodes after each test (see white zones in depth, at the beginning of the profile in Figures 4(a) and (b)), and inversion errors (see white zones just below the surface layer of strong increases in Figures 4(a)–(d)). The different theoretical scenarios established in this work, which are based on field study and the stratigraphic site characteristics, are a powerful tool for the greater understanding of this type of methodology in tropical zones because there is also a similarity between the pseudo-sections of apparent electrical resistivity and synthetic data.

## Acknowledgements

We want to thank the Laboratorio de Investigación en Ingeniería y Ciencias Aplicadas of the Centro Experimental de Ingeniería at the Universidad Tecnológica de Panamá (UTP in Spanish) for their logistical support. Also, we want to thank Jorge A. Espinosa, manager of the Hydrometeorological section at the Panama Canal Authority for the given meteorological data. Finally we would like to acknowledge the editorial services provided by Sustainable Sciences Institute (SSI), in particular the revisions and comments made by Eng. Dana Brock, an SSI volunteer.



## Author Contributions

Conceived and designed the experiments: AM, ID, CAH, FO. Analyzed the data: AM, ID, CAH. Wrote the first draft of the manuscript: AM, RP, JF. Contributed to the writing of the manuscript: FO, RP, JF. Agree with manuscript results and conclusions: DV, JH, AM, ID, CAH, FO, RP, JF. Jointly developed the structure and arguments for the paper: AM, ID, CAH, DV, RP, FO. Made critical revisions and approved final version: RP, JF. All authors reviewed and approved of the final manuscript.

## DISCLOSURES AND ETHICS

As a requirement of publication the authors have provided signed confirmation of their compliance with ethical and legal obligations including but not limited to compliance with ICMJE authorship and competing interests guidelines, that the article is neither under consideration for publication nor published elsewhere, of their compliance with legal and ethical guidelines concerning human and animal research participants (if applicable), and that permission has been obtained for reproduction of any copy-righted material. This article was subject to blind, independent, expert peer review. The reviewers reported no competing interests.

## REFERENCES

- Hubbard SS, Rubin Y. Introduction to Hydrogeophysics. In: Rubin Y, Hubbard SS, eds. *Hydrogeophysics*. The Netherlands: Springer; 2005:3–21.
- Williams JH, Lapham WW, Barringer TH. Application of electromagnetic logging to contamination investigations in glacial sand-and-gravel aquifers. *Groundwater Monitoring and Remediation Review*. 1993;13:129–138.
- Haeni FP. Use of ground-penetrating radar and continuous seismic-reflection profiling on surface-water bodies in environmental and engineering studies. *Journal of Environmental and Engineering Geophysics*. 1996;1:27–35.
- Annan AP. GPR Methods for Hydrogeological Studies. In: Rubin Y, Hubbard S, eds. *Hydrogeophysics*. The Netherlands: Springer; 2005:185–213.
- Steeple DW. Shallow Seismic Methods. In: Rubin Y, Hubbard S, eds. *Hydrogeophysics*. The Netherlands: Springer; 2005:215–251.
- Ekinci Y, Demirci A, Ertekin C. Delineation of the seawater-freshwater interface from the coastal alluvium of Kaleköy-Gökçeada, NW Turkey. *Journal of Applied Science*. 2008;8:1977–1981.
- Robinson DA, Binley A, Crook N, et al. Advancing process-based watershed hydrological research using near-surface geophysics: a vision for, and review of electrical and magnetic geophysical methods. *Hydrological Processes*. 2008; 22:3604–3635.
- Pellerin L. Applications of electrical and electromagnetic methods for environmental and geotechnical investigations. *Surveys in Geophysics*. 2002;23:101–132.
- Sandberg SK, Slater LD, Versteeg R. An integrated geophysical investigation of the hydrogeology of an anisotropic unconfined aquifer. *Journal of Hydrology*. 2002;267:227–243.
- Louis IF, Louis FI, Grambas A. Exploring for favorable groundwater conditions in hardrock environments by resistivity imaging methods: synthetic simulation approach and case study example. *Journal of Electrical & Electronics Engineering*. 2002;1–4.
- Louis IF, Vafidis AV, Louis FI, Tassopoulos N. The use of geophysical prospecting for imaging the aquifer of Lakka carbonates, Mandoudi Euboea, Greece. *Journal of the Balkan Geophysical Society*. 2002;5:97–106.
- Giudici M, Manera M, Romano E. The use of hydrological and geoelectrical data to fix the boundary conditions of ground water flow model: a case study. *Hydrology and Earth System Science*. 2003;7:297–303.
- Braga AC, Filho WM, Dourado JC. Resistivity (DC) methods applied to aquifer protection studies. *Brazilian Journal of Geophysics*. 2006;24:573–581.
- Robineau B, Join JL, Beauvais A, Parisot JC, Savin C. Geoelectrical imaging of a thick regolith developed on ultramafic rocks: groundwater influence. *Australian Journal of Earth Sciences*. 2007;54:773–781.
- Yeh TCJ, Lee CH, Hsu KC, Wen JC. Fusion of hydrologic and geophysical tomographic surveys. *Geosciences Journal*. 2008;12:156–167.
- Desclotres M, Ruiz L, Sekhar M, et al. Characterization of seasonal local recharge using electrical resistivity tomography and magnetic resonance sounding. *Hydrological Processes*. 2008;22:384–394.
- Chambers JE, Gunn DA, Wilkinson PB, et al. Non-invasive time-lapse imaging of moisture content changes in earth embankments using electrical resistivity tomography (ERT). In: Yu E, McDowell D, McDowell T, Editors. *Advances in Transportation Geotechnics*. 2008:475–480.
- Miller CR, Routh PS, Brosten TR, McNamara J. Application of time-lapse ERT imaging to watershed characterization. *Geophysics*. 2008;73:G7–G17.
- Clément R, Desclotres M, Günther T, Ribolzi O, Legchenko A. Influence of shallow infiltration on time-lapse ERT: Experience of advanced interpretation. *Geoscience*. 2009;34:886–898.
- Loke MH. *Res2Dmod ver. 3.01-Rapid 2D resistivity forward modelling using the finite-difference and finite-elements methods*. Technical Notes; 2002.
- Coates AG, Obando JA. The geologic evolution of the Central American isthmus. In: Jackson J, Coates A, eds. *Evolution and environment in tropical America*. Chicago: University of Chicago Press; 1996:21–56.
- Mann P. Geologic and tectonic development of the Caribbean plate boundary in southern Central America. *Oceanographic Literature Review*. 1996;43(11): 1116–1117.
- Jones SM. Geology of Gatun Lake and vicinity. *Geological Society of America Bulletin*. 1950;61:893–920.
- Terry RA. A geological reconnaissance of Panama. *California Academy of Sciences*. 1956;23:1–91.
- Woodring WP. *Geology and paleontology of Canal Zone and adjoining parts of Panama*. 1973; Washington: United States Department of the Interior.
- Stewart RH, Stewart JL, Woodring WP. *Geologic Map of Panama Canal and Vicinity, Republic of Panama*. Washington, DC: Department of the Interior, United States Geological Survey; 1980.
- Escalante G. The geology of southern Central America and western Colombia. In: Dengo G, Case J, Editors. *The Caribbean Region Boulder*. The Geological Society of America; 1990:201–230.
- Niedzialek JM. *Unusual Hydrograph Characteristics, Upper Río Chagres, Panama*. Storrs: University of Connecticut; 2007.
- Palka EJ. A geographic overview of Panama: Pathway to the continents and link between the seas. In: Harmon R, ed. *The Río Chagres, Panamá: A Multidisciplinary Profile of a Tropical Watershed*. The Netherlands: Springer; 2005:3–18.
- Nover G. Electrical properties of crustal and mantle rocks: A review of laboratory measurements and their explanation. *Surveys in Geophysics*. 2005;26:593–651.
- Barker RD. The application of time-lapse electrical resistivity tomography in groundwater studies. *The Leading Edge*. 1998;17:1454–1458.
- Loke MH, Barker RD. Least-squares deconvolution of apparent resistivity pseudosections. *Geophysics*. 1995;60:1682–1690.
- Loke MH. *Tutorial: 2-D and 3D electrical imaging surveys*. Technical Note; 2002.
- Advanced Geosciences, Inc. *Instruction Manual for EarthImager 2D (v. 2.4.0)*. 2009.
- Barker RD. *Principles of electrical imaging*. Research Note; 2001.
- Guérin R, Panissod C, Thiry M, et al. La friche industrielle de Mortagne-du-Nord (59)-III-Approche méthodologique d'étude géophysique non-destructive des sites pollués par des eaux fortement minéralisées. *Bull Soc Géol France*. 2002;173:471–477.
- Dey A, Morrison HF. Resistivity modelling for arbitrary shaped two-dimensional structures. *Geophysical Prospecting*. 1979;27:106–136.
- Karaoulis M, Tsouros P, Kim JH. Comparison of algorithms of time-lapse ERT inversion. *Geoelectrical Monitoring*. 2012;93:98–104.
- Pellicer XM, Zarroca M, Gibson P. Time-lapse resistivity analysis of Quaternary sediments in the Midlands of Ireland. *Journal of Applied Geophysics*. 2012;82:46–58.